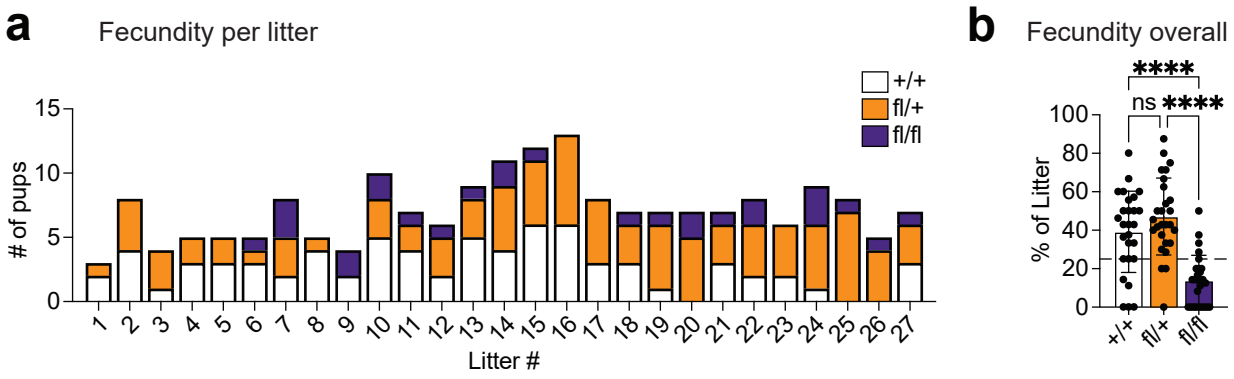
Extended Data Figures 1 – 8

Extended Data Fig. 1. *Csf1r*$^{Cre/+}$;*Wnk1*$^{fl/fl}$ mice do not follow Mendelian inheritance.

(a) Graph of litter size and genotype.

(b) Percentage of each litter distributed within each genotype. Legend: WT (white bars), Heterozygous (fl/+, orange bars), and Homozygous (fl/fl). Data shown as mean ± SD. Significance was determined via one-way ANOVA. ns = not significant. ****$p < .0001$.

Extended Data Fig. 1: *Csf1r*$^{Cre/+}$;*Wnk1*$^{fl/fl}$ mice do not follow Mendelian inheritance



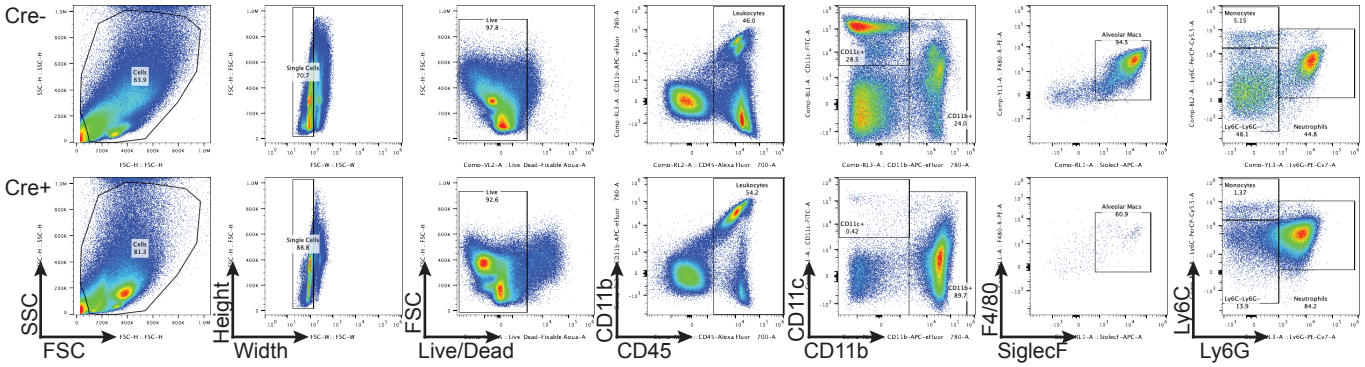
Extended Data Fig. 2. Tissue-resident macrophages are absent in essential organs.

(a) FACS gating scheme for **Figs. 1** and **3** and **Extended Data Fig. 2** and **7** using lung as an example. Data representative of 5 independent experiments.

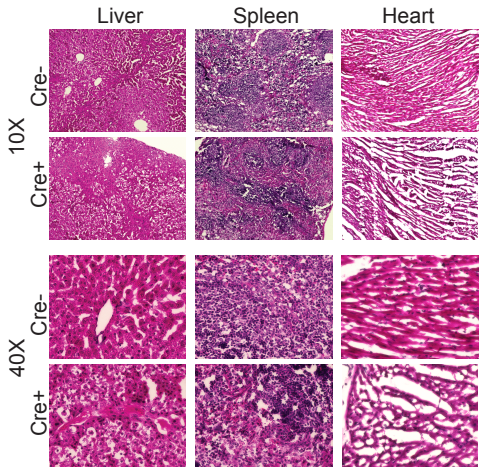
(b-d) Additional analyses of H&E, FACS, and IF data of obtained, analyzed, and presented as in **Fig. 1c,d**.

Supplementary Figure 2 **Tissue resident macropahges are absent in essential organs**

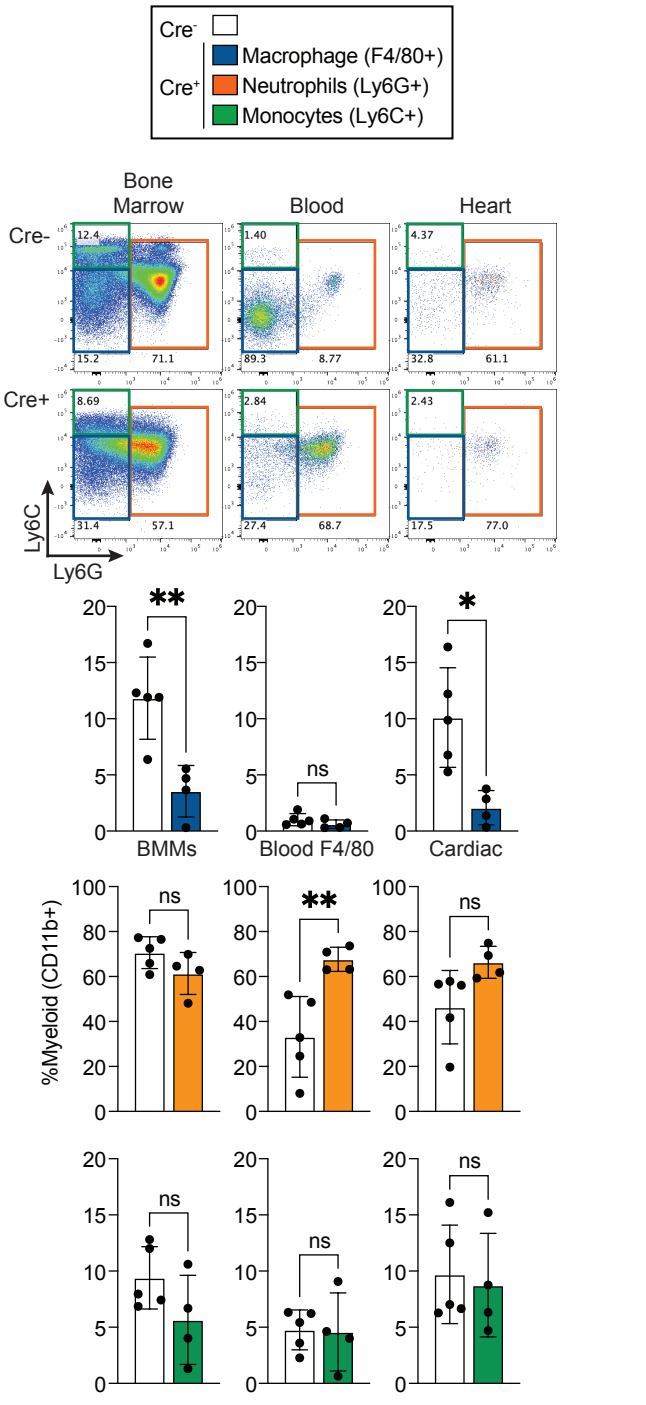
a Myeloid cell gating scheme (lung as example)



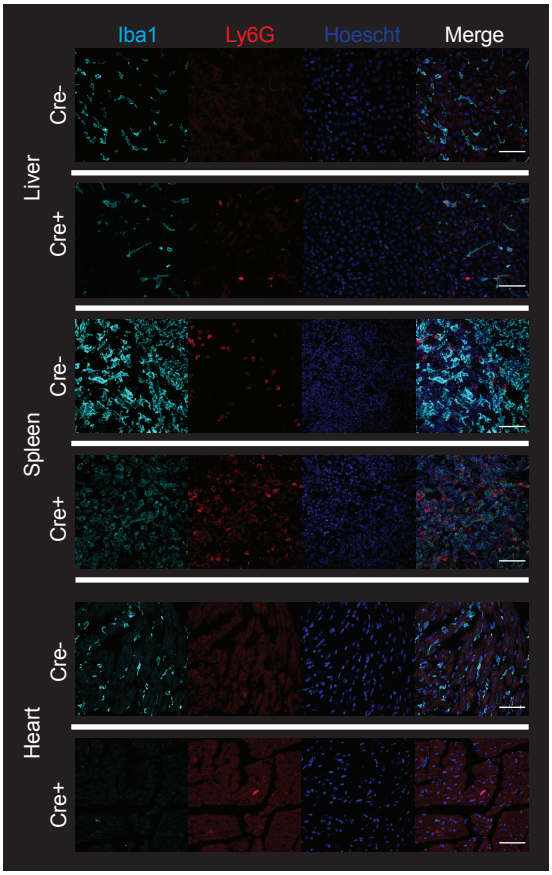
b H&E histology of Wnk1 KO organs



c Wnk1 KO myeloiod cell distribution in bone marrow, blood, and heart



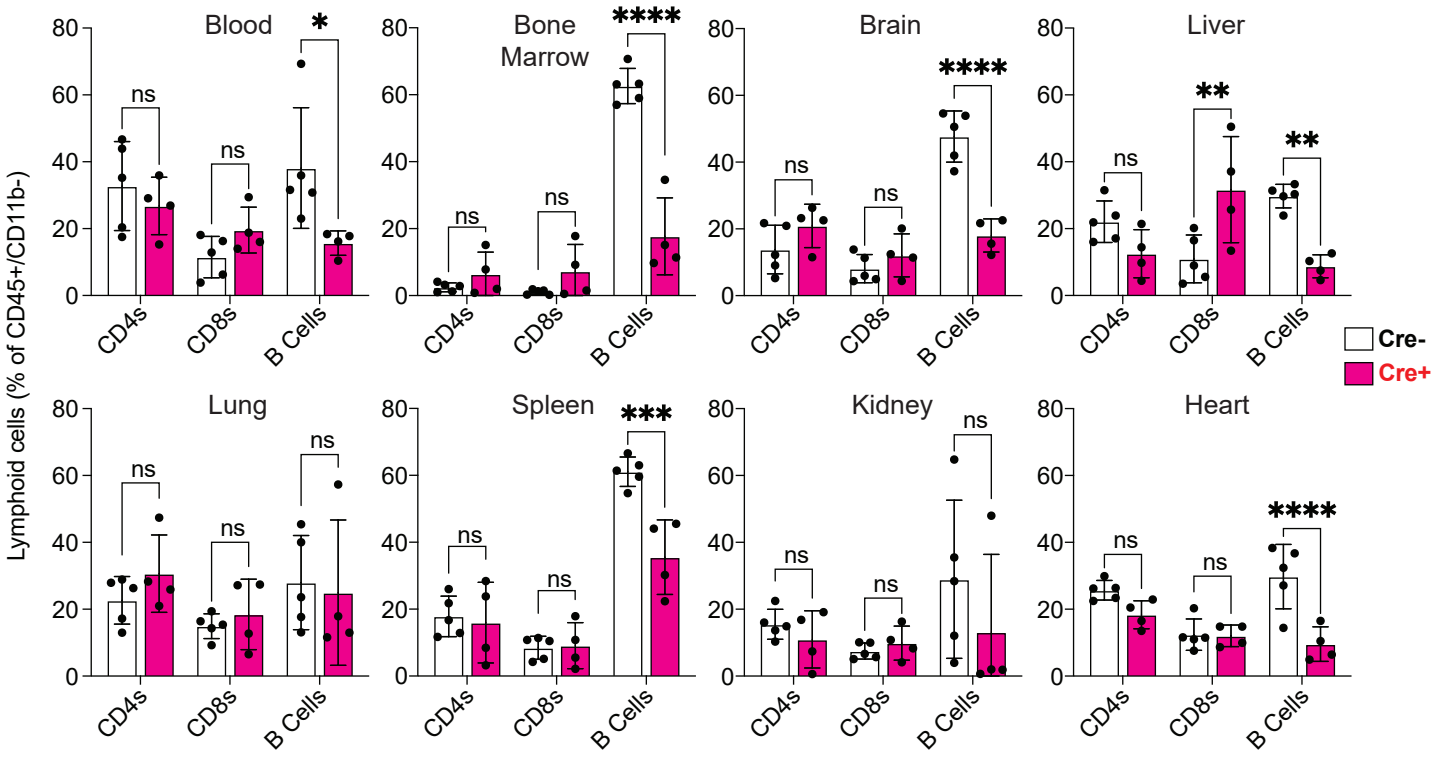
d Immunofluorescence of Wnk1 KO organs



Extended Data Fig. 3. Lymphoid cell distribution in major organs.

FACS analysis of lymphoid compartment in blood, bone marrow, brain, liver, lungs, spleen, kidney, and heart representing CD4 T cells (CD4+ CD8- CD19-), CD8 T cells (CD8+ CD4- CD19-), and B cells (CD19+ CD4- CD8-) gated on CD45+ CD11b- populations. Data shown as mean ± SD. Significance was determined via one-way ANOVA. ns = not significant. *$p < .05$, **$p < .01$, ***$p < .001$, ****$p < .0001$.

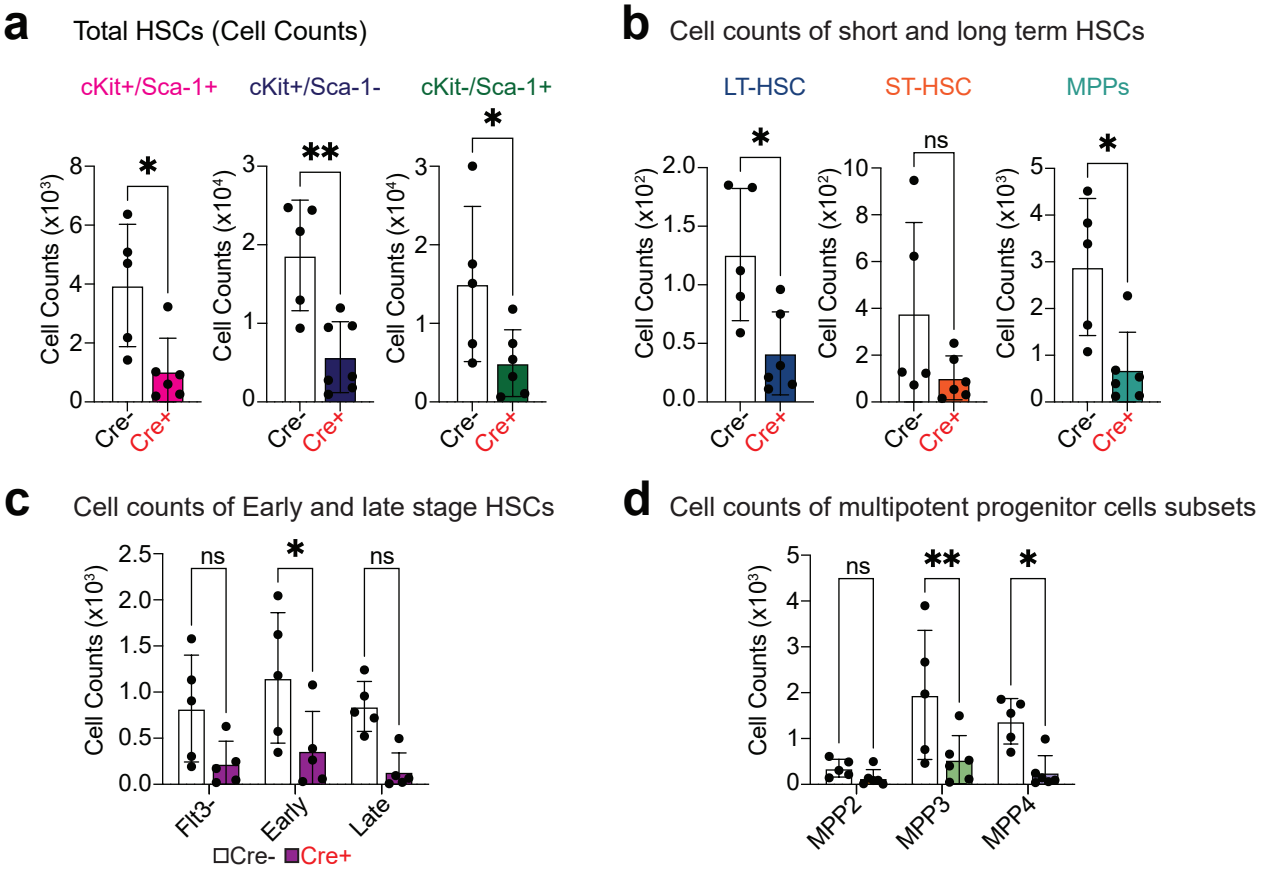
Extended Data Fig. 3: Lymphoid cell distribution in major organs



Extended Data Fig. 4. Total cell counts at different stages of hematopoiesis.

(a-d) Total cell counts according to flow cytometry counting beads for populations quantified in **Fig. 2b-e**. Cre-, n=5; Cre+, n=6. Data representative of 5 experiments pooled. **(a,b)** Data shown as mean ± SD with significance determined via independent samples *t*-test. ns = not significant. **p* < .05, ***p* < .01. **(c,d)** Data shown as mean ± SD. Significance was determined via one-way ANOVA. ns = not significant. **p* < .05, ***p* < .01.

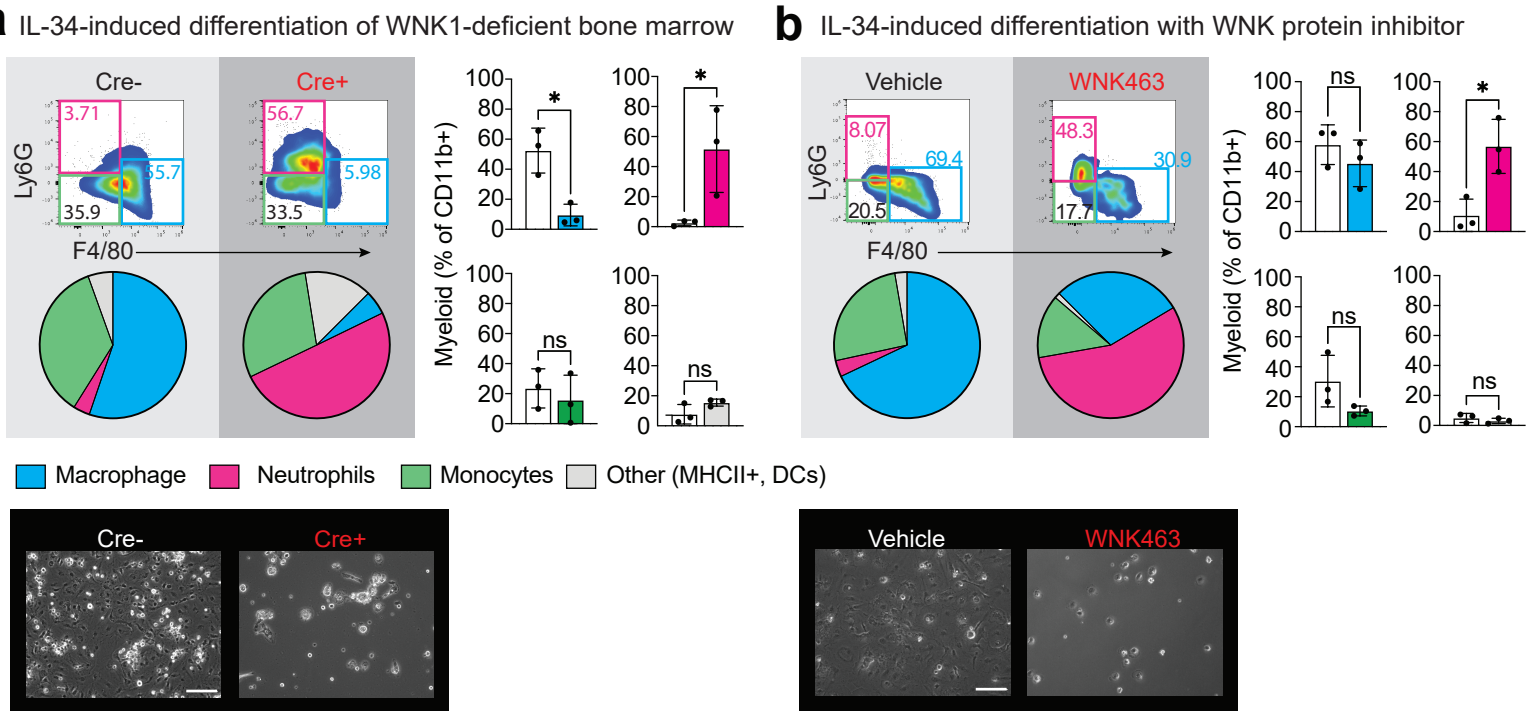
Extended Data Fig. 4: Total cell counts at different stages of hematopoiesis



Extended Data Fig. 5. WNK1 absence is not rescued by IL-34 stimulation.

(a,b) BMDMs cultured in 25ng/mL IL-34. Additional analysis of FACS data of BMDMs 7 days post isolation as in **Fig. 3a,b** and **Extended Data Fig. 5.** Bottom images obtained after 7 days in IL-34 of Cre- or Cre+ (left), and Vehicle or WNK463 treated (right). Scale bar, 150μm. n=3 per group. Data representative of 3 independent experiments. Data are shown as mean ± SD with significance determined via independent samples *t*-test. ns = not significant. **p* < .05, ***p* < .01.

Extended Data Fig. 5: WNK1 absence is not rescued by IL-34 stimulation

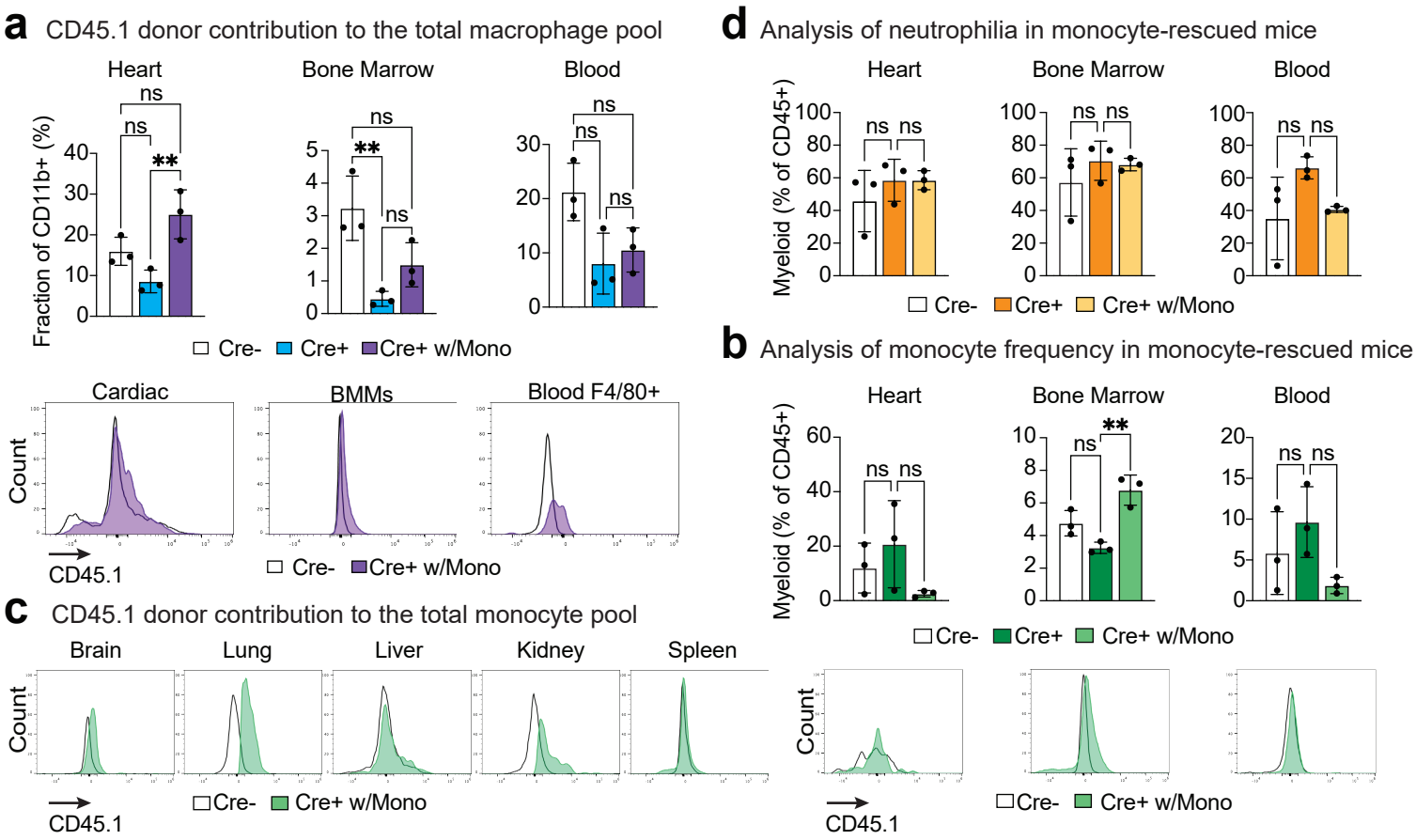


Extended Data Fig. 6. CD45.1 donor monocyte contribution in Cre+ recipient mice.

(a-c) FACS analysis of heart, BM, and blood in Cre-, Cre+, and Cre+ injected with donor monocytes obtained, analyzed, and presented as in **Fig. 3e-g**.

(d) CD45+ CD11b+ Ly6G- Ly6C+ monocytes from Cre-, Cre+, and Cre+ injected with donor monocytes and FACS analyzed for expression of CD45.1. Histograms show MFI of CD45.1 expression between Cre- (white) and Cre+ injected with donor monocytes (green). n=3 per group. Data are representative of 2 independent experiments. Data shown as mean ± SD. Significance was determined via one-way ANOVA. ns = not significant. $**p < .01$.

Extended Data Fig. 6: CD45.1 donor monocyte contribution in Cre+ recipient mice



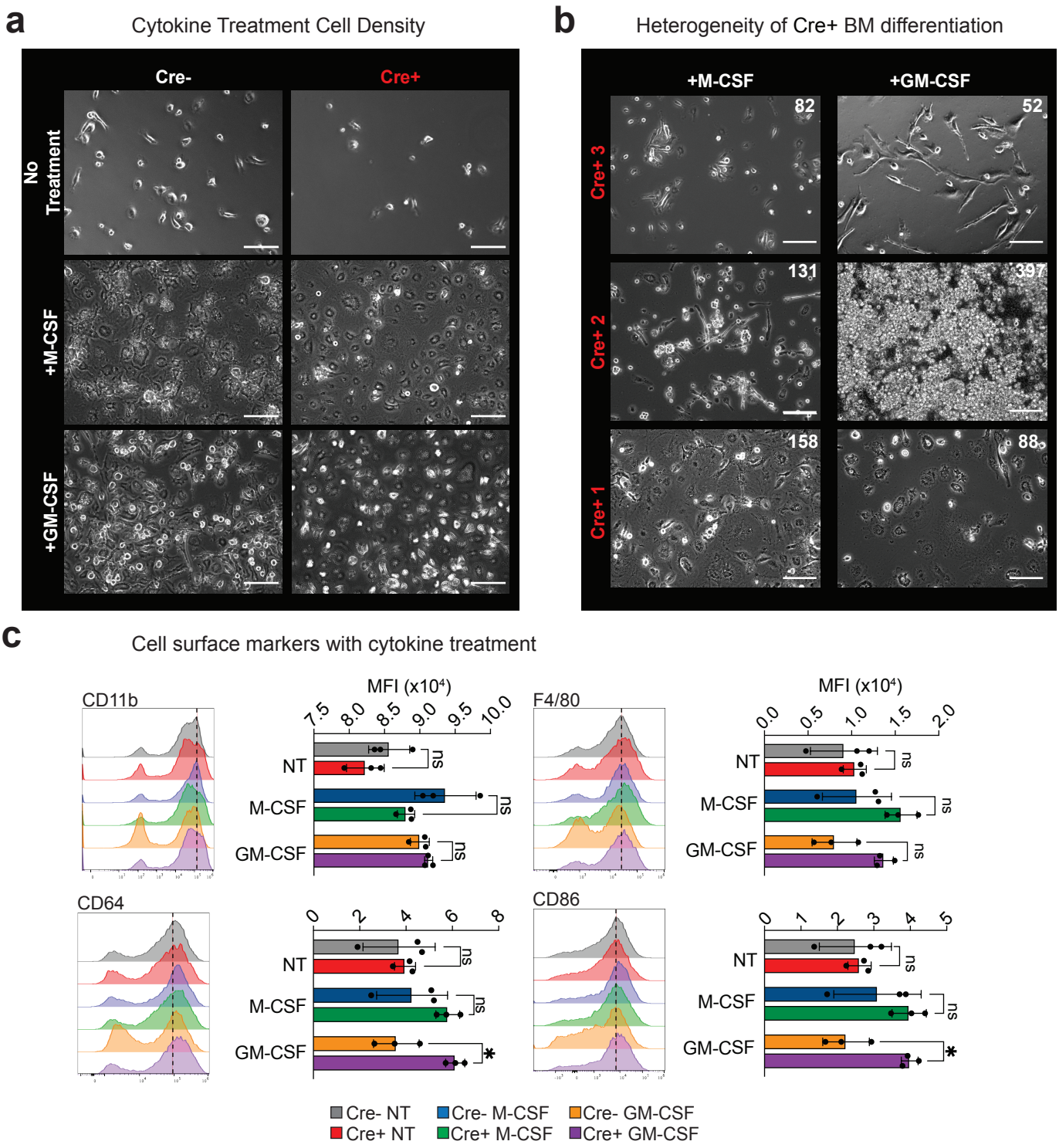
Extended Data Fig. 7. *Csf1r*$^{Cre/+}$;*Wnk1*$^{fl/fl}$ cells do not become conventional macrophages.

(a) Representative images of Cre- (left) and Cre+ (right) BMDMs differentiated without cytokines (top), 25ng/mL of M-CSF (middle), or 25ng/mL of GM-CSF (bottom) after 7 days in culture. Scale bars, 150μm.

(b) Images representing morphological heterogeneity of Cre+ cultures in M-CSF (left) and GM-CSF (right). White numbers in upper right denote total cell count from each well. Scale bars, 150μm.

(c) Representative histograms and quantification of FACS data plotting MFI of CD11b, CD64, CD86, and F4/80 from cells harvested from **(a)**. n=3 per group. Data representative of 3 experiments and shown as mean ± SD. With significance determined via one-way ANOVA. ns = not significant. *$p < .05$.

Extended Data Fig. 7: *Csf1r*$^{Cre/+}$*:Wnk1*$^{fl/fl}$ cells do not become conventional macrophages



Extended Data Fig. 8. WNK463 blocks human progenitor differentiation into macrophages.

(a) Representative images of monocytes isolated from human PBMCs and cultured for 5 days in the presence of 50ng/mL of M-CSF or GM-CSF with or without WNK463. Scale bars, 50μm (inlay, 20μm).

(b) Quantification of cell surface markers Csf1r (left) and CD206 (right) on human monocyte-derived macrophages as a frequency of CD11b+ myeloid cells differentiated for 5 days in M-CSF (cyan) or GM-CSF (magenta). n=2 healthy donors.

(c) Replicate images from **Fig. 4i** of human EBs treated with 50ng/mL human cytokines M-CSF and GM-CSF with or without WNK463 for 14 days. Scale bars, 50μm (inlay, 20μm).

(d) Histograms of FACS data plotting MFI of human cell surface markers CD14, CD11b, CD80, CD206, CD66b, CD11c, CD86, and HLA-DR from EBs harvested at day 7 from M-CSF (cyan) or GM-CSF (magenta) conditions.

(e,f) FACS analysis of human cell surface markers characterizing differentiation of iPSC-derived macrophages from EB-derived progenitors. **(e)** From left to right, histogram plots (top) and overlaid dot plots (bottom) of CD11b, HLA-DR, CD66b, CD86, CD11c, and CD206 from M-CSF (cyan) and M-CSF +WNK463 (light grey), and GM-CSF (magenta) and GM-CSF +WNK463 (dark grey). MFIs quantified in **(f)**. n=4-6 per group. Data represent 3 experiments and is shown as mean ± SD with significance determined via independent samples *t*-test. ns = not significant. **p* < .05, ***p* < .01, *****p* < .0001.

Extended Data Fig. 8: WNK463 blocks human progenitor differentiation into macrophages

